

# Peptide Network for Detection of Tissue-Remodeling Enzyme in the Prognosis of Hepatocellular Carcinoma

Yue Yu,<sup>†,‡</sup> Hao Li,<sup>‡</sup> Bin Zhang,<sup>§</sup> Xiaoshu Pan,<sup>‡</sup> Xiaoli Zhu,<sup>§</sup> Yitao Ding,<sup>\*,†</sup> and Genxi Li<sup>\*,‡,§</sup>

<sup>†</sup>Nanjing Drum Tower Hospital, The Affiliated Hospital of Nanjing University Medical School, Nanjing 210008, China

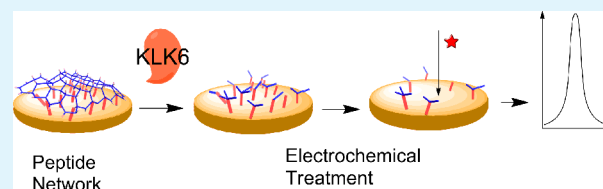
<sup>‡</sup>State Key Laboratory of Pharmaceutical Biotechnology, Department of Biochemistry, Nanjing University, Nanjing 210093, China

<sup>§</sup>Laboratory of Biosensing Technology, School of Life Sciences, Shanghai University, Shanghai 200444, China

## Supporting Information

**ABSTRACT:** In this work, a surface-confined peptide network that can exhibit distinct structural features under protease cleavage and electrochemical treatment is developed as a highly sensitive biosensor for clinical detection of kallikrein 6 (KLK6). KLK6 is a serine protease of the tissue-remodeling process determining the development of hepatocellular carcinoma (HCC). The peptide network, immobilized on the electrode surface by a Au–S bond, loses its integrity upon KLK6 cleavage and is removed from the electrode by electrochemical desorption of thiol groups, while the network without protease cleavage can remain attached by a few intact Au–S bonds. In this manner, distinct conductivity of the electrode surface in the presence/absence of protease can result in a large signal-to-background ratio, enabling KLK6 detection in clinical samples. The detected KLK6 abundance can manifest the correlation between up-regulated KLK6 activity and the progress of HCC. These results suggest a potential future use of this peptide network as a biosensor to provide diagnostic information for better administration of HCC.

**KEYWORDS:** peptide network, hepatocellular carcinoma, kallikrein 6, extracellular matrix, electrochemical detection



## 1. INTRODUCTION

Recently, peptide-based nanoassemblies<sup>1–5</sup> have enabled a range of new biosensor designs.<sup>6,7</sup> As an emerging targeting agent<sup>8</sup> for bioanalysis<sup>9–12</sup> and therapeutic development,<sup>13</sup> peptides can interact with many different targets ranging from proteins to synthetic drug compounds. Moreover, these interactions often involve a self-propagating mechanism, resulting in cascades of peptide-assembling/disassembling process.<sup>14</sup> Thus, employing such peptides as the building block of a biosensing nanoassembly, evident structural reconfiguration can be triggered by a very small amount of analyte. Taking these potential advantages of the peptide nanoassembly, we propose to construct a bioinspired nanoassembly mimicking the network formed by the various components of the extracellular matrix (ECM). Similar to the ECM, the peptide network can have modified morphology after interactions with various ECM enzymes. This process, known as tissue remodeling, was recently found to be essential to the development of hepatocellular carcinoma (HCC). HCC is one of the most common worldwide causes of cancer death, usually with a life expectancy of less than 1 year. This current difficulty in effectively managing HCC arises from its lengthy but unclear process of pathological development.<sup>15–17</sup> Recently, accumulating data characterize this process as a constant remodeling of the ECM around the hepatocyte, resulting in the final malignant transformation.<sup>18,19</sup> This malignant modification of ECM is the result of the active participation of various tissue remodeling enzymes. Therefore, elucidating the role of these

enzymes in the development of HCC may help to define new approaches toward better control of HCC, and great efforts have been made using conventional immunoanalysis. However, the overall expression level thus determined may prove less advantageous for analyzing a dynamic system as the ECM, since the cell signaling of the remodeling process may keep only part of the expressed enzymes in the bioactive state. Therefore, activity assays may lend more help to clarify the complicated interplay between tissue remodeling enzymes and the ECM in the development of HCC.

In this work, the proposed ECM mimicking peptide network is employed to design an activity assay of kallikrein 6 (KLK6),<sup>20</sup> a serine protease involved in the ECM modification of many cancers.<sup>21,22</sup> The peptide network is designed to contain the substrate sequence of KLK6. In ECM remodeling, KLK6 interacts more and more extensively with the ECM by gradually decomposing its components, finally giving rise to a passage for the invasion of tumor cells. Similarly, in the designed peptide network, interaction with KLK6 gradually disintegrates it in a self-propagating manner, since every KLK6 cleavage can expose more sites to subsequent cleavage. Moreover, by immobilizing the peptide network on the surface of an electrode, electrochemical treatment of the network can amplify the structural change caused by KLK6 cleavage. Employing in-solution

**Received:** December 18, 2014

**Accepted:** January 28, 2015

**Published:** January 28, 2015

electrochemical reporter, the low background in the absence of KLK6 can be coupled with the evident response after KLK6 cleavage, in a label-free manner, to enable a low limit of detection. The ability of the proposed method in quantitatively and specifically detecting active KLK6 is first verified using standard samples. Its application is then extended to clinical samples from HCC patients. The detected amount of active KLK6 can reliably indicate the degree of malignancy in the HCC clinical samples, since higher KLK6 activity can be detected in HCC of more advanced grade and stage, as well as greater power of metastasis. These results may point to the prospect of using the proposed method to provide prognostic information for the development and advancing of HCC.

## 2. EXPERIMENTAL SECTION

**2.1. Chemicals and Reagents.** Linker (dipenzylcyclooctyne-DDDWMTRSAMG-polyethylene glycol-WYMTRSAMGDDD-dipenzylcyclooctyne) and foothold (mercaptoundecanoic acyl-(azido)-G-GGG-(azido)G-GGG-(azido)G) peptides were synthesized by Shanghai Science Peptide Biological Technology Co., Ltd., as lyophilized powder, purity > 95%. Human recombinant KLK6 was from R&D system. Other reagents were of analytical grade. A powder of the peptide probe was dissolved to the desired concentration in 10 mM phosphate buffer solution (PBS) (pH 7.4). For all solutions, double-distilled water (ddH<sub>2</sub>O) was prepared in a Milli-Q purification system to 18 MΩ-cm. Biopsy samples from hepatocellular carcinoma patients were from the Department of General Surgery of the Nanjing Drum Tower Hospital after elected consent by the local ethical committee. All samples were retrieved from patients undergoing curative tumor excision, and adjacent normal tissue was also obtained for each patient as a control. The retrieved samples were immediately sliced on ice and fractionated with a nuclear extract kit obtained from Abnova.

**2.2. Electrode Treatment and Modification.** These steps were essentially the same as those previously reported,<sup>9</sup> except that after the foothold peptide had been immobilized on the electrode surface, 30 μM linker peptide in 10 mM PBS (pH 7.4) was incubated with the electrode for 10 min to form the network.

**2.3. KLK6 Assay.** The desired amount of KLK6 in 10 mM PBS (pH 7.4) was first activated by 1 mU/mL lysyl-endopeptidase for 30 min, before being incubated with the network-modified electrode for 60 min to cleave the linker peptides. After thorough rinsing with water and 5% tween-20, the electrode was subject to 0.1 V/s cyclic voltammetric scans for 10 cycles in 10 mM PBS (pH 7.4). After a subsequent rinsing step, the electrode was ready for measurement. In detecting clinical sample, the freshly fractionated sample was diluted 100× and activated by lysyl-endopeptidase and then brought to the same detection procedure just described.

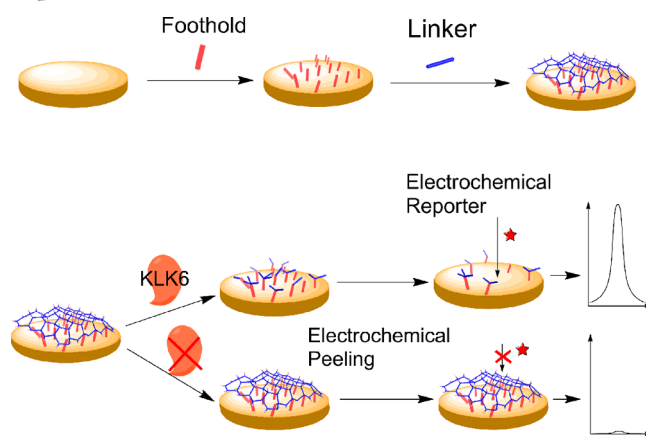
**2.4. AFM Measurement.** Atomic force microscopy (AFM) images were recorded using an ex situ Agilent 5500 AFM system. Samples were imaged at a scan rate of 0.5–1 Hz in tapping mode. AFM tips with a resonant frequency in the range 160–260 kHz were used. Images were acquired at a resolution of 512 × 512 pixels.

**2.5. Electrochemical Measurements.** These steps were essentially the same as those previously reported.<sup>9</sup> The measurements were conducted at room temperature using an electrolytic system composed of three electrodes: the modified gold electrode as the working electrode, the saturated calomel electrode as the reference electrode, and a platinum wire serving as the auxiliary electrode. All electrochemical measurements were done in deoxygenated buffer solutions. The data were obtained from at least three repetitions of independent experiments.

## 3. RESULTS AND DISCUSSION

Scheme 1 may illustrate the formation of the proposed biosensing network and its application in KLK6 detection. The network is formed by many surface-anchored foothold

**Scheme 1. Principle of the Designed KLK6 Assay Using Peptide Network (not drawn to scale)**



peptides interconnected by the linker peptides. Specifically, the linker peptide contains two KLK6 cleavage sites, spaced out by a polyethylene glycol (PEG) linker; while the two ends of the peptide are functionalized with copper-free clickable groups, dipenzylcyclooctyne. On the other hand, the foothold peptides, immobilized on the electrode via a Au–S bond, consist of azide groups, the counterpart of dipenzylcyclooctyne, on a flexible polyglycine chain. Employing click chemistry, a network of peptides can be formed on the electrode surface. During the detection procedure, cleavage of the network by KLK6 can be self-propagating, since every cleavage can expose more sites to subsequent cleavage. This cleavage destroys the integrity of the network, so the footholds are isolated from one another. To maximize the effect of KLK6 cleavage, electrochemical peeling via oxidative opening of the Au–S bond<sup>23</sup> is employed to uproot the footholds, thereby removing the isolated footholds together with the cleaved linkers. On the contrary, the network, in the absence of protease, can resist the electrochemical peeling, due to the fact that the network is immobilized by a great many redundant footholds. Therefore, although the attaching of the peptide network is weakened by electrochemical peeling, a few intact footholds can be sufficient for the whole interconnected network to remain attached to the electrode surface. After peeling, distinct surface structure in the presence/absence of KLK6 cleavage can give rise to evident signal/background contrast using the in-solution reporter  $[\text{Fe}(\text{CN})_6]^{3-/4-}$ .

The working principle of this design is first verified using electrochemical impedance spectra (EIS) and atomic force microscopy (AFM). As shown in Figure 1, EIS of the bare electrode appears as a straight line (line a) and subsequent immobilization of foothold peptides results in a semicircle (line b), indicating resistance to interface electron transfer due to the formation of peptide monolayer. After the network is formed, dramatic rising of the impedance is observed (line c), owing to both the spatial arrangement of the network and its strong electrostatic repulsion to  $[\text{Fe}(\text{CN})_6]^{3-/4-}$  originated from the large number of aspartic acids contained in the peptide. Furthermore, it can be observed in Figure 1 that the following two steps of KLK6 cleavage and electrochemical peeling evidently reduce the impedance (lines d and e), corresponding to disintegration of the network. On the contrary, in the absence of KLK6, the peeling step can have a negligible influence on the impedance (line f), indicating that the intact network remains attached. The surface morphology of the

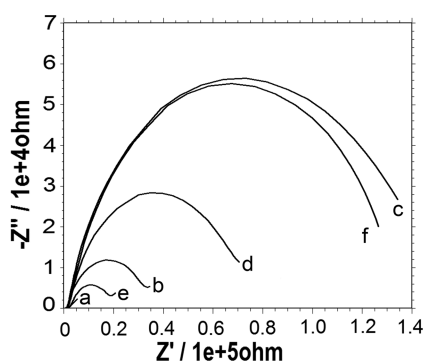


**Figure 1.** Stepwise electrochemical impedance spectra (EIS) recorded in the KLK6 assay (KLK6 concentration 10 nM).

network undergone in the above steps is also observed with AFM. As shown in Figure S1, Supporting Information, shortly after adding KLK6 to the network, a lot of bright patches representing the protease can be found on the surface of interconnected thin threads, representing the linkers. Beneath this layer, a lot of spots can be observed, representing the foothold peptides (Figure S1a, Supporting Information). Figure S1b, Supporting Information, reveals that subsequent cleavage removes many linkers together with the protease. After that, the electrochemical desorption step almost completely clears the surface of foothold and linker peptides (Figure S1c, Supporting Information).

To obtain a better performance of the peptide network-based biosensor, the spatial arrangement of the network is studied and optimized. First, the surface density of the foothold peptides is evaluated (Figure S2, Supporting Information), and on average, each foothold is separated from the neighboring one by 10–20 nm, sufficient for the linker (1–5  $\mu\text{m}$ ) to form an interconnected assembly. Second, the number of azide groups on the foothold peptide is optimized (Figure S3, Supporting Information), and it is known that 3 azide groups per foothold are sufficient to produce a densely interwoven linker network with a low background. Third, to find a proper surface density of the linker, its concentration for assembly is optimized (Figure S4, Supporting Information). As can be expected, a concentration higher than the certain threshold (near 30  $\mu\text{M}$ ) can achieve no lower background, other than lowering signal response, since too many densely connected linkers may hamper KLK6 cleavage. Thus, 30  $\mu\text{M}$  is chosen as the standard

linker concentration. The optimized network is then employed to study cleavage time for KLK6 detection; 60 min is found to be enough for cleavage (Figure S5, Supporting Information). Subsequently, the electrochemical treatment is optimized. The electrochemical peeling treatment, acting in contrast to linker concentration, can give higher signal response at the expense of the signal:background ratio. The potential range for the electrochemical peeling is first investigated (Figure S6, Supporting Information). The scans of broader potential range tend to desorb more peptides in the absence of KLK6 cleavage, resulting in higher background signal; therefore, a relatively small scan range from  $-0.7$  to  $-1.2$  V is employed for the subsequent experiments. Then the effects of repetitive voltammetric scans with a different number of cycles are compared. As shown in Figure S7, Supporting Information, a peeling step with 10 cycles of voltammetric scans is found to result in a balanced readout with high response and low background. Besides, it has also been verified that the lysyl-endopeptidase employed to activate KLK6 has no evident effect on the background signal (Figure S8, Supporting Information).

Under the optimized conditions, the peptide network-based biosensor may have a response linearly proportional to the logarithm of KLK6 concentration, with a limit of detection (LOD) less than 1 pM (Figure 2). The LOD and dynamic range can fulfill the requirement of serum detection, since the borderline of KLK6 as serum cancer biomarker is in the micromolar to nanomolar range.<sup>21</sup> Further experiments reveal that the average variance of all repetitive measurements is less than 5% ( $n = 3$ ), showing good reproducibility. Moreover, several control targets, such as HSA, abundant in serum, and KLK 3/PSA, another member of KLK family, can only have background signal (Figure 3). Thus, the specificity can be satisfactory.

KLK6 has a broad spectrum of tissue expression and has been established as the serum marker for various cancers. However, the activity of KLK6 is mostly observed in tissue, especially during the tissue remodeling process in embryonic and cancerous development. For many types of cancer, recent reports have suggested an intimate connection between up-regulated KLK6 activity and the remodeling of ECM.<sup>24</sup> Besides, it has also been suggested that the development of HCC is sustained and guided by the microenvironment of the malignantly transformed hepatocytes.<sup>19</sup> In this cancerous microenvironment, the activity of many ECM enzymes is up-regulated to create a niche suitable for the growth and invasion

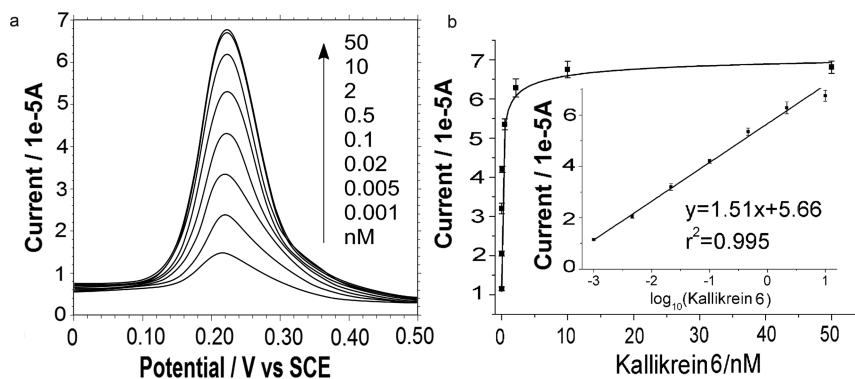


**Figure 2.** (a) Square wave voltammograms (SWVs) of  $[\text{Fe}(\text{CN})_6]^{3-/4-}$  for quantifying KLK6. (b) Calibration curve of SWV peak response in a as a function of KLK6 concentration; (inset) linear relationship between the logarithm of KLK6 concentration and signal response; error bars represent standard deviation ( $n = 3$ ).

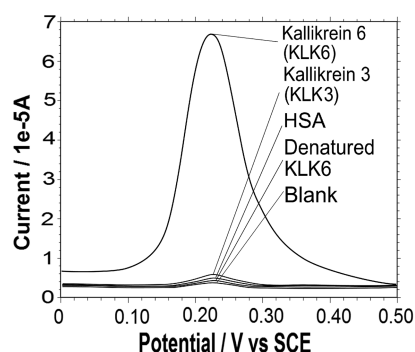


**Figure 3.** SWVs showing specificity of the assay. All targets are at 10 nM.

of HCC. These observations point to the possibility of KLK6-facilitated malignant transformation and tumor invasion in HCC, and this can be manifested in a parallel in KLK6 activity and the advancing of HCC. To investigate this potential correlation, histologically examined samples of hepatocellular cancer are fractionated, and the cellular KLK6 expression is determined using the peptide network. The detected KLK6 abundance from 15 victims is grouped according to grade, TNM stage, and extent of metastasis. By all the groupings statistically significant elevation of KLK6 expression can be found in advanced cases (Figure 4), suggesting a closely related KLK6 function with the progress of HCC, consistent with the result and extrapolation of previous reports.<sup>25</sup>

#### 4. CONCLUSION

A biosensing peptide network has been developed as a highly sensitive biosensor for clinical detection of KLK6, based on the self-propagated and electrochemically facilitated structural rearrangement of the network. The distinct behavior of the network in the presence/absence of the protease combines low background and prominent signal response to yield a LOD less than 1 pM as well as a satisfactory dynamic range. In terms of sensitivity and detection range, this method has outperformed the commercially available ELISA methods, which helps to realize the clinical KLK6 detection. The determined KLK6 abundance in hepatocellular carcinoma is found to parallel cancer development, pointing to a future usage of this peptide

network as a biosensing nanosystem for cancer screening and prognostic guidance.

#### ■ ASSOCIATED CONTENT

##### Supporting Information

Surface characterization of the surface-immobilized peptide network and optimization of various experimental conditions. This material is available free of charge via the Internet at <http://pubs.acs.org>.

#### ■ AUTHOR INFORMATION

##### Corresponding Authors

\*E-mail: [drdingyitao@sina.com](mailto:drdingyitao@sina.com).

\*E-mail: [genxili@nju.edu.cn](mailto:genxili@nju.edu.cn).

##### Notes

The authors declare no competing financial interest.

#### ■ ACKNOWLEDGMENTS

This work was supported by the National Natural Science Foundation of China (Grant No. 21235003) and the National Science Fund for Distinguished Young Scholars (Grant No. 20925520).

#### ■ REFERENCES

- (1) Lamb, B. M.; Luo, W.; Nagdas, S.; Yousaf, M. N. Cell Division Orientation on Biospecific Peptide Gradients. *ACS Appl. Mater. Interfaces* **2014**, *6*, 11523–11528.
- (2) Kim, S. J.; Park, M. H.; Moon, H. J.; Park, J. H.; Ko, D. Y.; Jeong, B. Polypeptide Thermogels as a Three Dimensional Culture Scaffold for Hepatogenic Differentiation of Human Tonsil-Derived Mesenchymal Stem Cells. *ACS Appl. Mater. Interfaces* **2014**, *6*, 17034–17043.
- (3) Shi, Y. P.; Yi, C. Q.; Zhang, Z. M.; Zhang, H.; Li, M. J.; Yang, M. S.; Jiang, Q. Peptide-Bridged Assembly of Hybrid Nanomaterial and Its Application for Caspase-3 Detection. *ACS Appl. Mater. Interfaces* **2013**, *5*, 6494–6501.
- (4) Cui, H. G.; Cheetham, A. G.; Pashuck, E. T.; Stupp, S. I. Amino Acid Sequence in Constitutionally Isomeric Tetrapeptide Amphiphiles Dictates Architecture of One-Dimensional Nanostructures. *J. Am. Chem. Soc.* **2014**, *136*, 12461–12468.
- (5) Xu, X. H.; Jian, Y. T.; Li, Y. K.; Zhang, X.; Tu, Z. X.; Gu, Z. W. Bio-Inspired Supramolecular Hybrid Dendrimers Self-Assembled from Low-Generation Peptide Dendrons for Highly Efficient Gene Delivery and Biological Tracking. *ACS Nano* **2014**, *8*, 9255–9264.

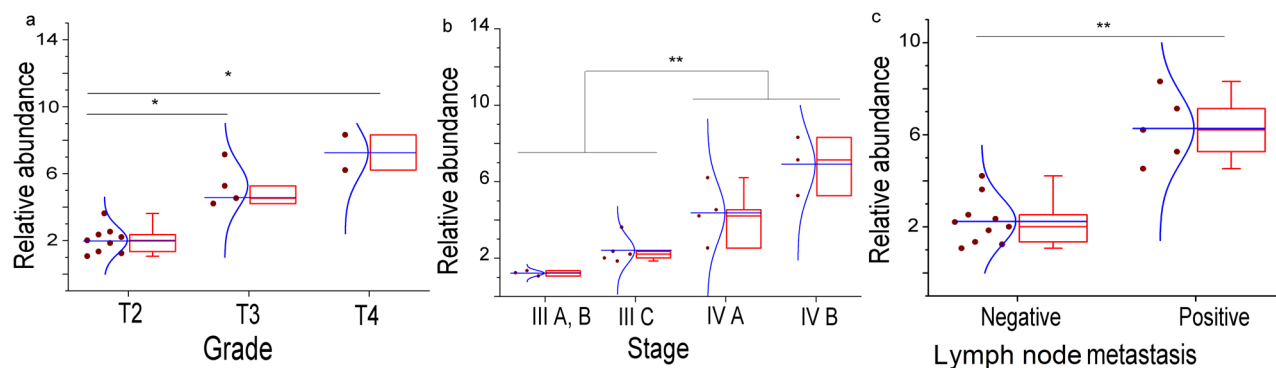


**Figure 4.** Box charts to show the distribution of KLK6 abundance in 15 patients of HCC, examined with the proposed method. (a) Patients are grouped according to the grade of HCC, (b) patients are grouped according to the stage of HCC, and (c) patients are grouped according to the presence or absence of metastasis. For each sample, the detected KLL6 in cancerous tissue is normalized by that in the adjacent normal tissue. Raw data is included as a column scatter plot to the left of each box. A curve corresponding to the normal distribution is also displayed on top of the scatter plot. Statistical significance of the observed difference between groups is accessed by the *t* test: \**P* < 0.05; \*\**P* < 0.01.

- (6) Hao, Y. Q.; Zhou, B. B.; Wang, F. B.; Li, J.; Deng, L.; Liu, Y. N. Construction of Highly Ordered Polyaniline Nanowires and Their Applications in DNA Sensing. *Biosens. Bioelectron.* **2014**, *52*, 422–426.
- (7) Khatayevich, D.; Page, T.; Gresswell, C.; Hayamizu, Y.; Grady, W.; Sarikaya, M. Selective Detection of Target Proteins by Peptide-Enabled Graphene Biosensor. *Small* **2014**, *10*, 1505–1513.
- (8) Mascini, M.; Palchetti, I.; Tombelli, S. Nucleic Acid and Peptide Aptamers: Fundamentals and Bioanalytical Aspects. *Angew. Chem., Int. Ed.* **2012**, *51*, 1316–1332.
- (9) Li, H.; Xie, H. N.; Cao, Y.; Ding, X. R.; Yin, Y. M.; Li, G. X. A General Way to Assay Protein by Coupling Peptide with Signal Reporter via Supramolecule Formation. *Anal. Chem.* **2013**, *85*, 1047–1052.
- (10) Li, H.; Xie, H. N.; Yang, N. N.; Huang, Y.; Sun, L. Z.; Li, G. X. Design of a Bi-functional Peptide for Protein Assays: Observation of Cortactin Expression in Human Placenta. *Chem. Commun.* **2013**, *49*, 5387–5389.
- (11) Li, H.; Xie, H.; Huang, Y.; Bo, B.; Zhu, X.; Shu, Y.; Li, G. Highly Sensitive Protein Detection Based on a Novel Probe with Catalytic Activity Combined with a Signal Amplification Strategy: Assay of MDM2 for Cancer Staging. *Chem. Commun.* **2013**, *49*, 9848–9850.
- (12) Li, H.; Huang, Y.; Zhang, B.; Yang, D.; Zhu, X.; Li, G. A New Method to Assay Protease Based on Amyloid Misfolding: Application to Prostate Cancer Diagnosis Using a Panel of Proteases Biomarkers. *Theranostics* **2014**, *4*, 701–707.
- (13) Ruoslahti, E. Peptides as Targeting Elements and Tissue Penetration Devices for Nanoparticles. *Adv. Mater.* **2012**, *24*, 3747–3756.
- (14) Leckie, J.; Hope, A.; Hughes, M.; Debnath, S.; Fleming, S.; Wark, A. W.; Ulijn, R. V.; Haw, M. D. Nanopropulsion by Biocatalytic Self-Assembly. *ACS Nano* **2014**, *8*, 9580–9589.
- (15) Arzumanyan, A.; Reis, H.; Feitelson, M. A. Pathogenic Mechanisms in HBV- and HCV-associated Hepatocellular Carcinoma. *Nat. Rev. Cancer* **2013**, *13*, 123–135.
- (16) Baffy, G.; Brunt, E. M.; Caldwell, S. H. Hepatocellular Carcinoma in Non-Alcoholic Fatty Liver Disease: an Emerging Menace. *J. Hepatol.* **2012**, *56*, 1384–1391.
- (17) Sun, B. C.; Karin, M. Obesity, Inflammation, and Liver Cancer. *J. Hepatol.* **2012**, *56*, 704–713.
- (18) Fridman, W. H.; Pages, F.; Sautes-Fridman, C.; Galon, J. The Immune Contexture in Human Tumours: Impact on Clinical Outcome. *Nat. Rev. Cancer* **2012**, *12*, 298–306.
- (19) Leonardi, G. C.; Candido, S.; Cervello, M.; Nicolosi, D.; Raiti, F.; Travali, S.; Spandidos, D. A.; Libra, M. The Tumor Microenvironment in Hepatocellular Carcinoma. *Int. J. Oncol.* **2012**, *40*, 1733–1747.
- (20) Emami, N.; Diamandis, E. P. Utility of Kallikrein-Related Peptidases (Klks) as Cancer Biomarkers. *Clin. Chem.* **2008**, *54*, 1600–1607.
- (21) Diamandis, E. P.; Scorilas, A.; Fracchioli, S.; van Gramberen, M.; de Bruijn, H.; Henrik, A.; Soosaipillai, A.; Grass, L.; Yousef, G. M.; Stenman, U. H.; Massobrio, M.; van der Zee, A. G. J.; Vergote, I.; Katsaros, D. Human Kallikrein 6 (Hk6): A New Potential Serum Biomarker for Diagnosis and Prognosis of Ovarian Carcinoma. *J. Clin. Oncol.* **2003**, *21*, 1035–1043.
- (22) Santin, A. D.; Diamandis, E. P.; Bellone, S.; Soosaipillai, A.; Cane, S.; Palmieri, M.; Burnett, A.; Roman, J. J.; Pecorelli, S. Human Kallikrein 6: a New Potential Serum Biomarker For Uterine Serous Papillary Cancer. *Clin. Cancer Res.* **2005**, *11*, 3320–3325.
- (23) Wildt, B.; Wirtz, D.; Searson, P. C. Triggering Cell Detachment from Patterned Electrode Arrays by Programmed Subcellular Release. *Nat. Protoc.* **2010**, *5*, 1273–1280.
- (24) Ghosh, M. C.; Grass, L.; Soosaipillai, A.; Sotiropoulou, G.; Diamandis, E. P. Human Kallikrein 6 Degrades Extracellular Matrix Proteins and May Enhance the Metastatic Potential of Tumour Cells. *Tumor Biol.* **2004**, *25*, 193–199.
- (25) Lu, L.; Yang, Z.; Zhu, B.; Fang, S.; Yang, X.; Cai, W.; Li, C.; Ma, J. X.; Gao, G. Kallikrein-Binding Protein Suppresses Growth of Hepatocellular Carcinoma by Anti-Angiogenic Activity. *Cancer Lett.* **2007**, *257*, 97–106.